

# RSC Advances



This is an *Accepted Manuscript*, which has been through the Royal Society of Chemistry peer review process and has been accepted for publication.

*Accepted Manuscripts* are published online shortly after acceptance, before technical editing, formatting and proof reading. Using this free service, authors can make their results available to the community, in citable form, before we publish the edited article. This *Accepted Manuscript* will be replaced by the edited, formatted and paginated article as soon as this is available.

You can find more information about *Accepted Manuscripts* in the [Information for Authors](#).

Please note that technical editing may introduce minor changes to the text and/or graphics, which may alter content. The journal's standard [Terms & Conditions](#) and the [Ethical guidelines](#) still apply. In no event shall the Royal Society of Chemistry be held responsible for any errors or omissions in this *Accepted Manuscript* or any consequences arising from the use of any information it contains.

# Ionic Tagged Amine Supported on Magnetic Nanoparticles: Synthesis and Application in the Versatile Catalytic Knoevenagel Condensation in Water

Anguo Ying \*, Fangli Qiu , Chenglin Wu , Huanan Hu, Jianguo Yang \*

*(School of Pharmaceutical and Chemical Engineering, Taizhou University, Taizhou 318000)*

**Abstract:** Propylamine modified with imidazolium ionic moiety grafted onto the magnetic nanoparticles (MNPs) was prepared and evaluated as catalyst for Knoevenagel condensation in water at room temperature. The catalyst was efficient to the reaction to achieve the condensation products in good yields. It is noteworthy that the ionic tagged catalyst performed much better than the ionic-free counterpart. Finally, the catalyst could be reused for 8 times with slight loss of its catalytic activity.

**Keywords:** Magnetic nanoparticles, ionic tag, Knoevenagel condensation, recyclability.

## 1. Introduction

The Knoevenagel condensation of aldehydes with acidic active methylene compounds represents one of the most fundamental carbon-carbon formation reactions in the field of the organic transformations[1-6]. The corresponding condensation products are electrophilic trisubstituted alkenes, which have been widely used not only as starting materials for Michael addition[7], many domino or one-pot reactions[8], but also as important intermediates for the preparation of functional polymers, fine chemicals and pharmaceutical drugs[9]. Traditionally, these type of condensation reactions perform in homogeneous solution in presence of organic bases as well as their salts as catalysts, including dimethylamino pyridine, piperidine, guanidine, ethylenediamine[10]. These methods are obviously limited by the difficulties of catalyst

---

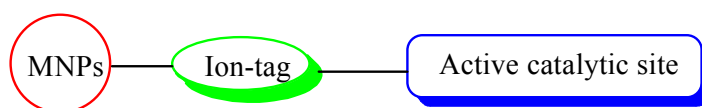
\* Corresponding authors. Tel/fax: +86 576 88660359.

E-mail address: [agyng@tzc.edu.cn](mailto:agyng@tzc.edu.cn) or [yinganguo@163.com](mailto:yinganguo@163.com) (A. Ying), [yjg@tzc.edu.cn](mailto:yjg@tzc.edu.cn) (J. Yang).

separation and recyclability. Therefore, many methodologies for Knoevenagel condensation catalyzed by heterogeneous catalysts were developed, in which the catalysts are readily recoverable and recycled. For examples, MgO/ZnO[11a], amine-functionalized polyacrylonitrile fiber[11b,c], La<sub>2</sub>O<sub>3</sub>/MgO[11d], Ni-SiO<sub>2</sub>[11e], Si-MCM-41 supported basic materials[11f] and IRMOF-3[11g] have been tested to catalyze the condensation reactions. Each of the above method has its own merit with at least one of the limitations of low yields, narrow substrate scope, harsh reaction conditions and the involvement of large amount of harmful, toxic organic solvents. Hence, improved methods for Knoevenagel condensation using inexpensive and readily available catalysts, less scavenger reagents coupled with easier work-up procedures are still highly desirable.

Magnetic nanoparticles (MNPs) are extensively studied as efficient supports to immobilize homogeneous catalysts for various organic transformations because of their interesting properties such as high surface area, paramagnetic properties, facilitating their separation from the reaction media after magnetization with an external permanent magnetic field [12]. MNPs-supported guanidine was developed and used to catalyze the cyanosilylation of carbonyl compounds with good to high yields of desired products achieved [13]. And the nanocatalyst can be reused up to 20 times. Gawande and coworkers reported a sulfonic acid catalyst grafted on magnetite and was subsequently served as an highly efficient magnetically catalyst for the Ritter and multicomponent reactions [14]. Meanwhile, a new concept of ion-tag strategy that can be achieved by installing an ionic substituent on the catalyst structure has been presented [15]. Catalysts optimized and designed according with the ion-tag strategy have three advantages, including water compatible, readily recycle and higher catalytic activities compared to the parent tag-free catalysts, which is, to

some extent, a working hypothesis. Thus, a series of novel ionic tagged catalysts have been emerged and exploited in versatile organic transformations, such as aza-Michael addition [16], selective hydroformylation [17], olefin reduction [18], Suzuki-Miyaura reaction [19], asymmetric Henry reaction [20], enantioselective  $\alpha$ -aminoxylations of ketones and aldehydes [21], asymmetric allylic etherification [22], and asymmetric addition [23]. Based on the unique properties of magnetic nanoparticle support and ion tag of ionic liquid, a new model for the design of efficient and recoverable catalysts has been developed via the combination of magnetite and ionic liquid (Scheme 1). Consequently, with the principal for the construction of catalysts in hand and in continuation of our research endeavors on development of environmental benign and sustainable chemical processes [24], herein, we report a novel MNPs supported amine with ionic tag and its application as a highly efficient and magnetically recoverable catalyst for versatile Knoevenagel condensation.



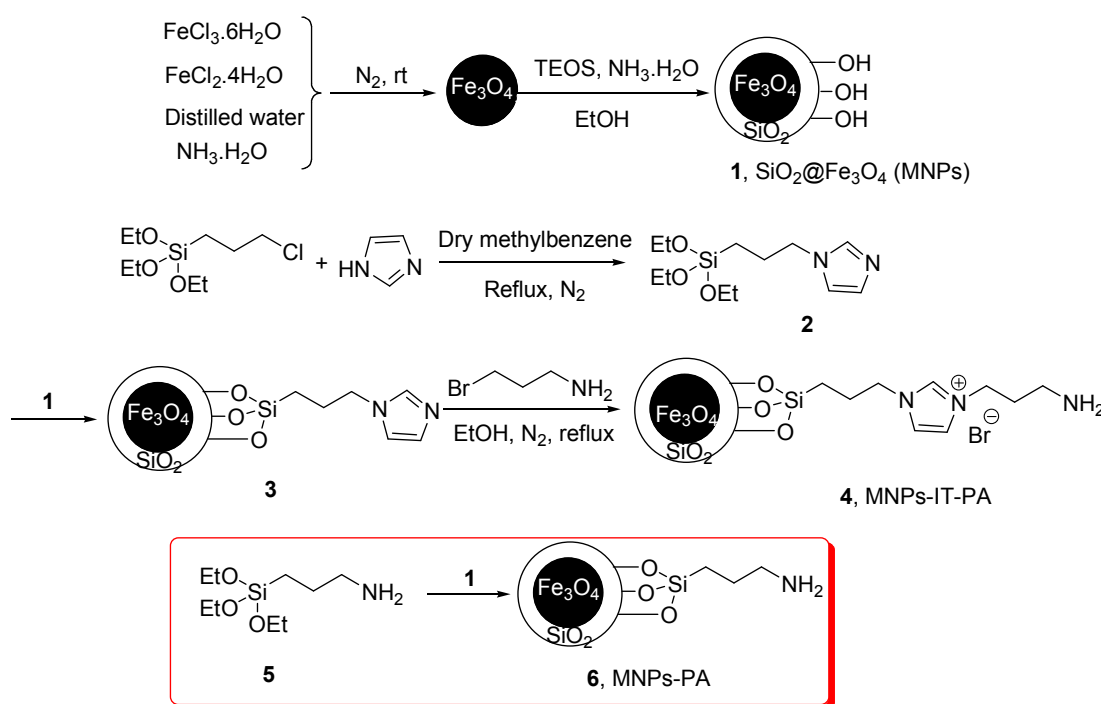
**Scheme 1** A model for design of novel catalysts

## 2. Results and discussion

### 2.1 Preparation and characterization of catalysts

The magnetic nanoparticle supported catalyst **4** (MNPs-IT-PA) was prepared through multiple steps from several commercially available chemicals (Scheme 2).  $\text{SiO}_2@\text{Fe}_3\text{O}_4$  **1** (MNPs) was synthesized by a chemical co-precipitating method reported by literatures [25], followed by silica coating [26]. The outer silica shell can not only prevent the aggregation of nanoparticles but also provide suitable surface Si-OH groups for further functionalization [27].

*N*-(3-propyltriethoxysilane) imidazole **2** was prepared via the condensation of imidazole and 3-chloropropyltriethoxysilane, then was grafted on the MNPs to give the supported imidazole **3**. Subsequently, **3** was treated with 3-bromine propylamine in dry toluene under reflux conditions at nitrogen atmosphere to afford the final catalyst MNPs-IT-PA **4**. For comparison, ion-free counterpart **6** (MNPs-PA), in which 3-aminopropyltriethoxysilane **5** was directly immobilized onto the magnetic nanoparticles, was prepared as outlined in Scheme 2.



**Scheme 2** Preparation of magnetic nanoparticle supported catalyst MNPs-IT-PA **4** and MNPs-PA

**6.**

The transmission electron microscopy (TEM) images in Fig.1 shows that MNPs (a), MNPs-PA (b) and MNPs-IT-PA (c) are of uniform-sized magnetic nanoparticles with almost spherical morphology. The diameter of the all three kinds of particles is approximately 16 nm, which is much larger than naked  $\text{Fe}_3\text{O}_4$  particles. The similar size and morphology of blank support (a) and amine anchored (b,c) means that the immobilization process did not change the magnetic ferrite core

and the modification reaction for catalyst loading only occurred on the silica shell surface.

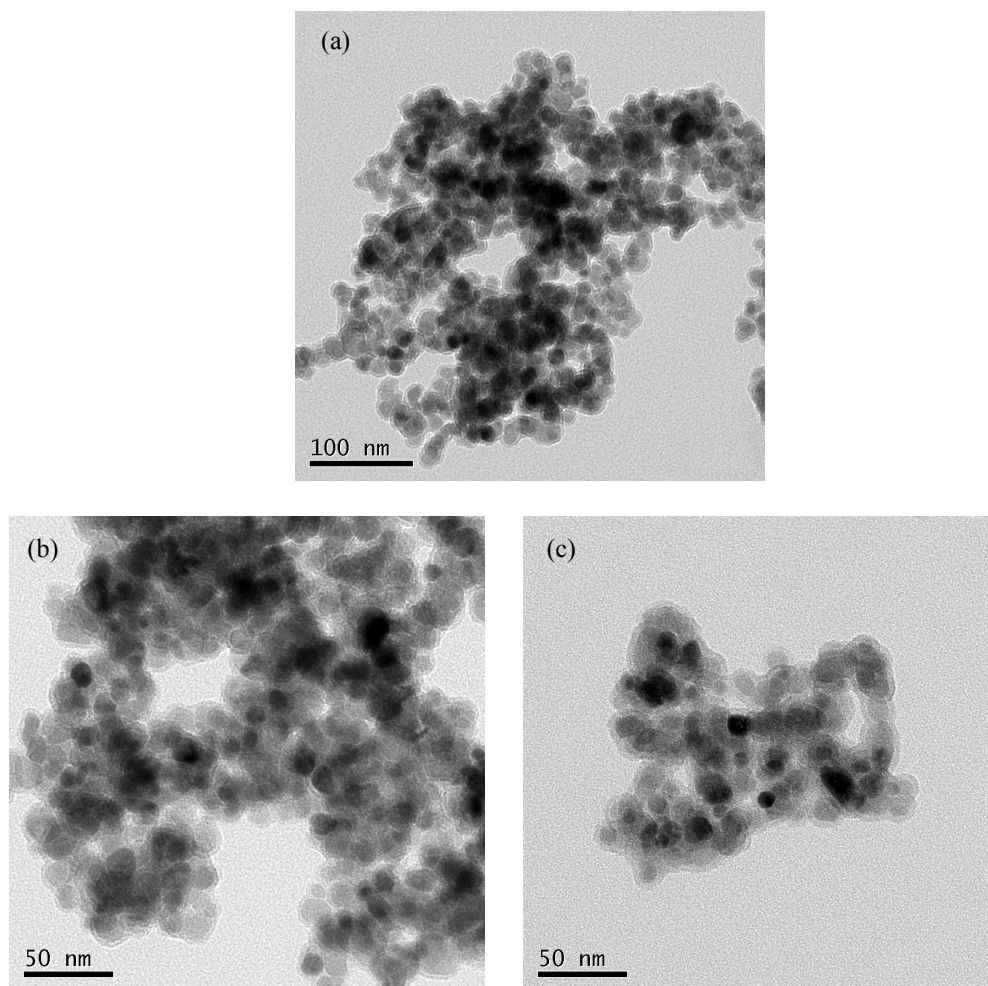


**Fig.1** TEM pattern of MNPs (a), MNPs-PA (b) and MNPs-IT-PA (c).

The X-ray diffraction (XRD) spectrums of anchored catalysts MNPs-IT-PA, MNPs-PA and MNPs have the same typical peaks regarding position and relative intensities (Fig.2). The broad peak from  $2\theta=18^\circ$  to  $28^\circ$  is attributed to the amorphous silica shell formed surrounding the  $\text{Fe}_3\text{O}_4$  core [28]. The peaks at  $30.07^\circ$ ,  $35.41^\circ$ ,  $43.04^\circ$ ,  $53.39^\circ$ ,  $56.91^\circ$ , and  $62.49^\circ$ , corresponding to the (220), (311), (400), (422), (511), and (440) reflections of the crystalline cubic spinel structure of standard naked  $\text{Fe}_3\text{O}_4$  sample (JCPDS 19-0629). As shown in Fig.2, the phase composition of

MNPs remained intact after surface modification operation on nanoparticles.

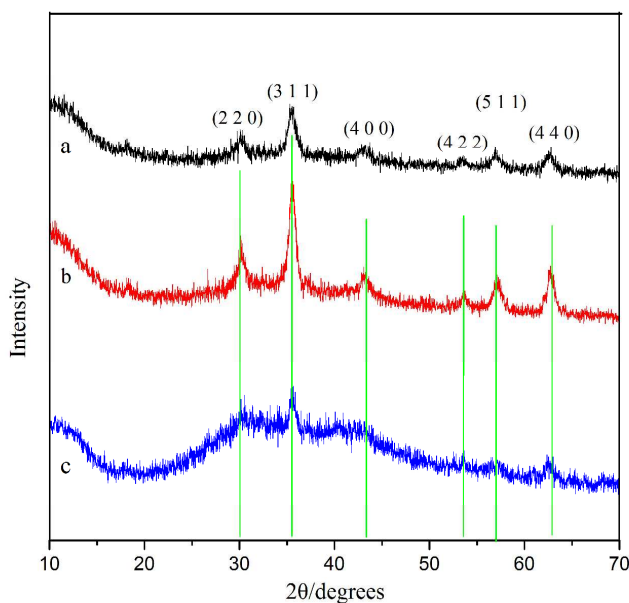


**Fig.2** XRD spectrums of MNPs (a), MNPs-PA (b) and MNPs-IT-PA (c).

Successful functionalization of the MNPs can be verified from the FT-IR spectrum in Fig.2.

In Fig.2, the band at  $579\text{ cm}^{-1}$  was assigned the characteristic Fe-O vibrations and could be confirm the existence of  $\text{Fe}_3\text{O}_4$  component in all three samples. A broad peak at around  $3400\text{ cm}^{-1}$  is attributed to the Si-OH group. Moreover, the presence of Si-O bond in three samples is evident from two characteristics vibrations at  $953\text{ cm}^{-1}$  and  $1086\text{ cm}^{-1}$ . The samples b and c have adsorptions at  $2965\text{ cm}^{-1}$ ,  $2874\text{ cm}^{-1}$ , and  $1465\text{ cm}^{-1}$ , examined as the C-H stretching vibration of linker 3-chloropropyltriethoxysilane anchored on the surface of  $\text{SiO}_2@\text{Fe}_3\text{O}_4$  [29]. The imidazole tag was responsible for the covalent anchoring of propylamine by forming an imidazolium-based ionic liquid moiety, which was evident from the characteristics bands at  $1507\text{ cm}^{-1}$  of C=N vibration and at  $3143\text{ cm}^{-1}$  of C-H stretching on the imidazole ring [30], as shown in Fig.3(c). Another two new bands at  $1211\text{ cm}^{-1}$  and  $1153\text{ cm}^{-1}$  corresponding to N-H stretching vibration of

primary amine indicated that the MNPs possessed propylamine modified by imidazolium ionic liquid.

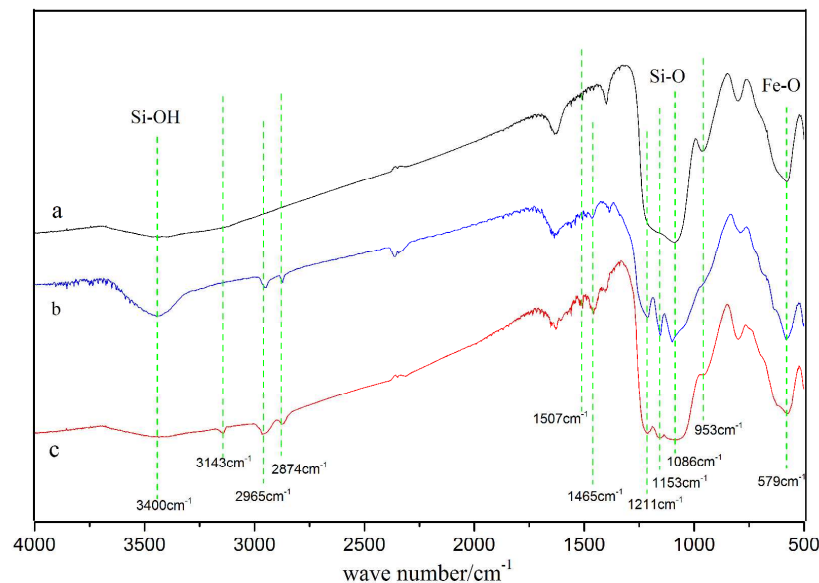


**Fig.3** FT-IR spectrums of MNPs (a), MNPs-PA (b) and MNPs-IT-PA (c).

The magnetic properties of neat  $\text{SiO}_2@Fe_3O_4$  (a), ionic-free supported amine (b) and ionic tagged amine anchored on MNPs (c) were investigated at room temperature (Fig.4). The saturation magnetizations were 32.2, 36.4, and 56.4 emu/g, respectively. It should be noted that still shows the high magnetization and superparamagnetism of the ionic tagged amine loaded sample exhibit well magnetic responsible and re-disperse properties, which enables the catalyst to be well dispersed in reaction solution and to be easily recovered by an external magnetic force (Fig.5).

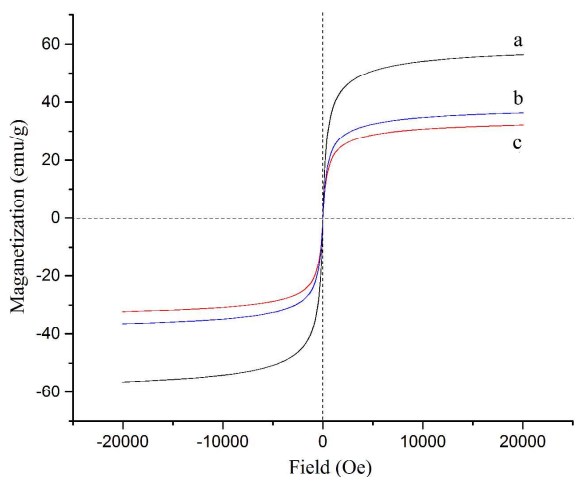


**Fig.4** Room temperature magnetization curves for MNPs (a), MNPs-PA (b) and MNPs-IT-PA (c).

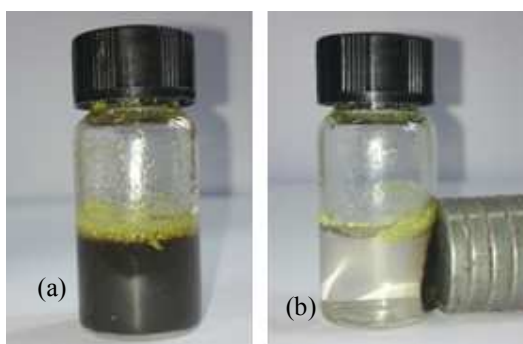


**Fig.5** Photographs of the dispersion of catalyst MNPs-IT-PA (a) and the separation of the catalyst with an external magnet.

The thermal stabilities of the two immobilized catalysts were determined by the thermogravimetric (TG) analysis. The results are shown in Fig.6. The two TG curves were divided into several regions corresponding to different mass loss ranges. The first weight loss for both samples, which occurred below 200 °C was probably due to the loss of the adsorbed solvent or trapped water on the surface and the structural water within amorphous silica outside of the Fe<sub>3</sub>O<sub>4</sub> core. A mass loss of approximately 4.5 % regarding SiO<sub>2</sub>@Fe<sub>3</sub>O<sub>4</sub>-PA occurred between 198 °C and 510 °C that was likely attributed to the loss of propylamine. The further mass loss of the

catalyst MNPs-PA at higher temperature resulted from the decomposition of silica shell (Fig.6a) [31]. As for catalyst MNPs-IT-PA, the second weight loss at the range of 199 °C to 350 °C accounted for the cleavage of imidazolium ionic liquid modified amine, which was very obvious in the DTG curve (Fig.6b). The occurrence of further decomposition beyond 351 °C could be designated as the complete loss of imidazolium-functionalized trialkoxysilane moiety [32]. The loading amount of propylamine and amine combined with ionic moiety were determined to be respectively 0.21 mmol/g, 0.34 mmol/g by elemental analysis, in well accordance with the TG analysis.

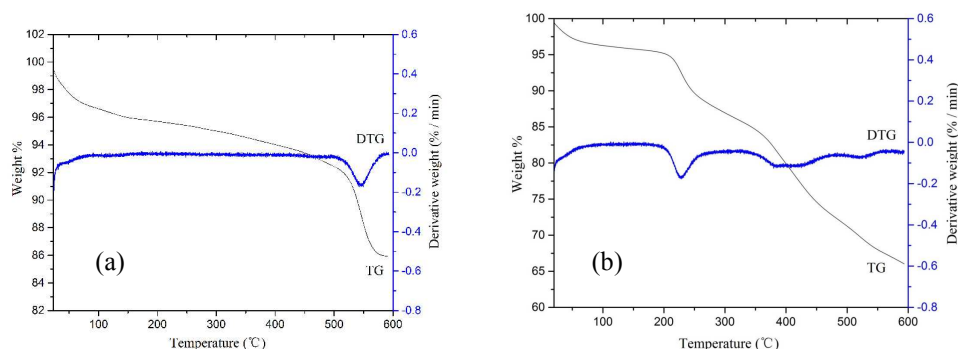


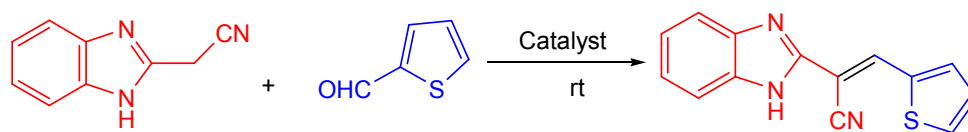
**Fig.6** TG-DTG analysis for SiO<sub>2</sub>@Fe<sub>3</sub>O<sub>4</sub>-PA(a) and MNPs-IT-PA (b).

## 2.2 Catalytic performances in versatile Knoevenagel condensation

The catalytic activities of MNPs-PA and MNPs-IT-PA were investigated using the Knoevenagel condensation between 2-(cyanomethyl)benzimidazole (5 mmol) and 2-thenaldehyde (5 mmol). As the results provided in Table 1, the catalyst MNPs-IT-PA performed well to give the desired product in within 2 h in 79 % yield, while ionic-free catalyst MNPs-PA gave the same desired product in 62 % yield (Table 1, entries 2 and 3). The compared result confirmed that MNPs-IT-PA catalyze the model reaction much better than the counterpart ionic-free MNPs-PA, which may be attributed the improved mass transfer originating from hydrophobic ionic moiety [33]. Only 28 %

yield of product was obtained when the reaction was carried out in the presence of a blank support ( $\text{SiO}_2@\text{Fe}_3\text{O}_4$ ) even if the reaction time was prolonged to 5 h (Table 1, entry 1). The reaction conditions were further optimized with different catalyst loadings, revealing that 5 mol % of catalyst MNPs-IT-PA afforded the best catalytic efficiency in terms of reaction rate and yield (Table 1, entries 4-7). For comparison, several organic solvents were also exploited as media for the reaction. The reactions catalyzed by MNPs-IT-PA in methanol, toluene and dichloromethane led to the product with lower yields (Table 1, entries 8, 10 and 12). It is noteworthy that the IL-free catalyzed performed better in organic solvents than the IL-tagged catalyst MNPs-IT-PA (Table 1, entries 8-13). Considering the reaction efficiency as well as the principal of green chemistry, the reaction catalyzed by MNPs-IT-PA in water at room temperature was used for further examinations.

**Table 1** Evaluation of the effects of the catalyst and solvent on the Knoevenagel condensation reaction of 2-(cyanomethyl)benzimidazole and 2-thenaldehyde at room temperature



Entry	Catalyst (mol %)	Solvent (10 mL)	Time (h)	Yield (%) <sup>a</sup>
1	MNPs ( $\text{SiO}_2@\text{Fe}_3\text{O}_4$ ) (73.5 mg)	$\text{H}_2\text{O}$	5	28
2	MNPs-PA (5.0)	$\text{H}_2\text{O}$	2	62
3	MNPs-IT-PA (5.0)	$\text{H}_2\text{O}$	2	79
4	MNPs-IT-PA (10.0)	$\text{H}_2\text{O}$	2	79
5	MNPs-IT-PA (20.0)	$\text{H}_2\text{O}$	3	80
6	MNPs-IT-PA (2.0)	$\text{H}_2\text{O}$	2	63

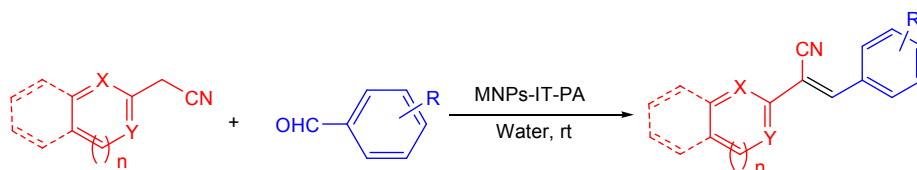
7	MNPs-IT-PA (0.5)	H <sub>2</sub> O	3	37
8	MNPs-IT-PA (5.0)	Methanol	3	58
9	MNPs-PA (5.0)	Methanol	2	68
10	MNPs-IT-PA (5.0)	Toluene	3	52
11	MNPs-PA (5.0)	Toluene	3	65
12	MNPs-IT-PA (5.0)	CH <sub>2</sub> Cl <sub>2</sub>	3	57
13	MNPs-PA (5.0)	CH <sub>2</sub> Cl <sub>2</sub>	3	61

<sup>a</sup> Isolated yield .

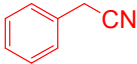
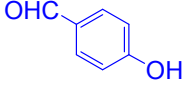
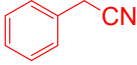
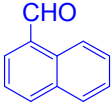
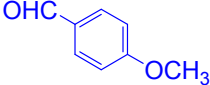
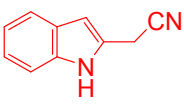
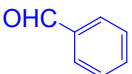
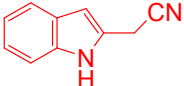
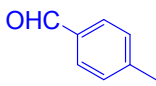
With the optimal reaction conditions in hand, we then proceeded to investigate the scope of methyl active compounds and various substituted arylaldehydes. The results are shown in Table 2. A wide range of aromatic aldehydes underwent reaction with 2-(cyanomethyl)benzimidazole in high yields (Table 2, entries 1-7). The reaction rate of aldehydes with electron-withdrawing group at the aromatic ring is slightly faster than that with electron-donating groups (Table 2, entries 1-2 vs. 3-6). On the other side, the reaction of mono-, di-, tri-substituted or 9-anthraldehyde proceeded more slowly than that of benzaldehyde due to the steric hindrance of the substituents at the ring (Table 2, entries 1 vs. 3-5 and 7). Gratifying, 2-(cyanomethyl)benzothiazole, phenylacetonitrile and indole-2-acetonitrile were also found to be efficient methylene active ingredients to give the desired condensation products in good yields albeit with relatively longer reaction times required regarding indole-2-acetonitrile (Table 2, entries 15 and 16). It is worthy to note that all the products obtained were *E*-geometry exclusively.

**Table 2** MNPs-IT-PA catalyzed Knoevenagel condensation of various aromatic aldehydes with

2-(cyanomethyl)benzimidazole, 2-(cyanomethyl)benzothiazole and phenylacetonitrile and indole-2-acetonitrile<sup>a</sup>

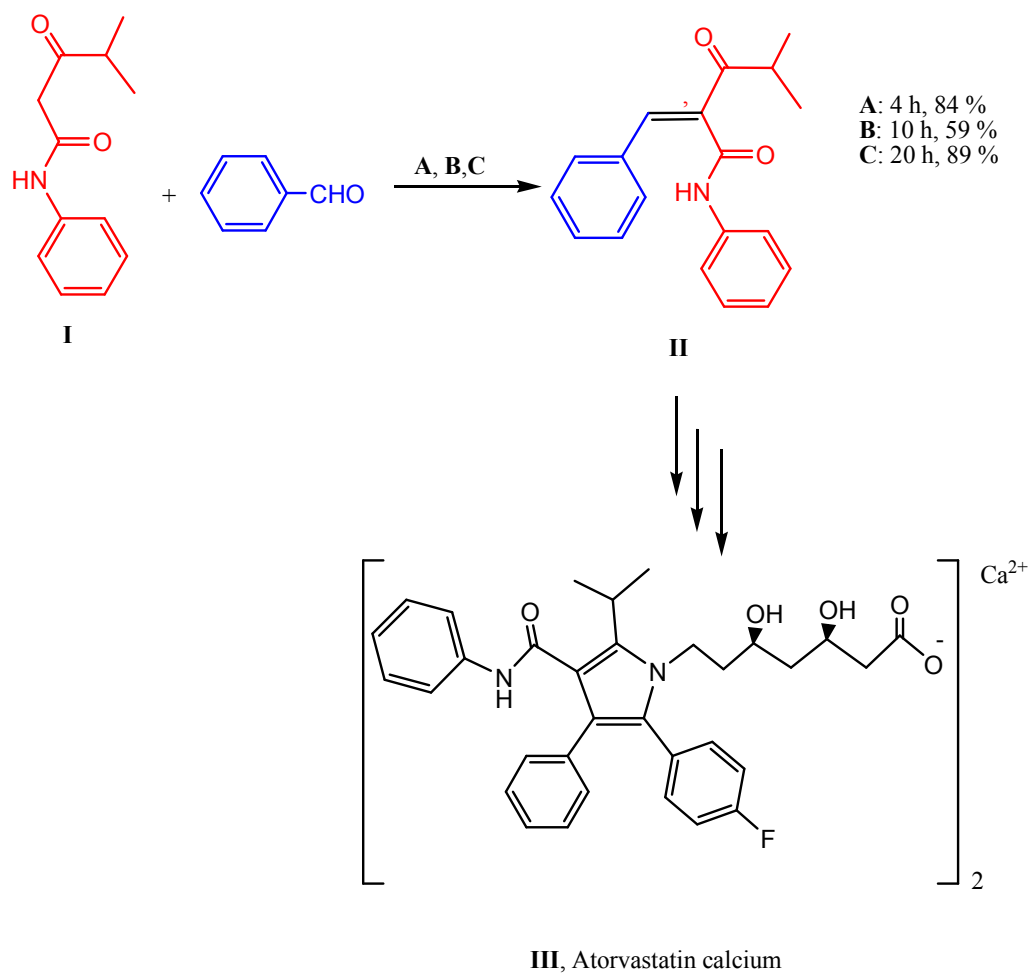


Entry	Substrate	Aldehyde	Time (h)	Yield (%) <sup>b</sup>
1			2	83
2			1.5	85
3			1	88
4			2	84
5			4	83
6			2	80
7			3	76
8			1.5	84
9			2	85
10			2	85
11			3	90

12			3	78
13			3	85
14			5	82
15			5	86
16			5	81

<sup>a</sup> Reaction conditions: methyl active compounds (5 mmol), aldehydes (5 mmol), water (10 mL), MNPs-IT-PA (5 mol %), rt. <sup>b</sup> Isolated yield.

Encouraged by the exciting results of cyano substituted methylene active compounds in the present catalytic system, herein, we also attempted to conduct the condensation of non-cyano substituted ketone (**I**) and benzaldehyde to give the product 4-methyl-3-oxo-*N*-phenyl-2-(phenylmethylene)pentanamide (**II**), which is a key intermediate for the preparation of Atorvastatin calcium (**III**), with the treatment function to inhibit 3-hydroxy-3-methylglutaryl-coenzyme (HMG-CoA) reductase (Scheme 3) [34]. To our pleasure, the reaction proceeded smoothly in the presence of catalyst MNPs-IT-PA in water and 84 % yield of product (**II**) was achieved within 4 h (Reaction conditions **A** in Scheme 3). Only 59 % product yield was obtained when the reaction was promoted by ionic tag-free catalyst SiO<sub>2</sub>@Fe<sub>3</sub>O<sub>4</sub>-PA (Conditions **B**). The traditional method for preparation **III** required large amount of organic solvent and acid (Conditions **C**). Compared with **B** and **C**, the reaction conditions **A** using ionic tagged MNPs-IT-PA as catalyst may provide a environmentally friendly alternative route for the synthesis of Atorvastatin calcium in industrial scale.



A: Ambient reaction catalyzed by MNPs-IT-PA in water at 80 °C

B: Reaction catalyzed by MNPs-PA in water at 80 °C

C: Reaction catalyzed by  $\beta$ -alanine and acetic acid in hexane at reflux condition.

**Scheme 3** Aqueous Knoevenagel condensation of non-cyano substituted ketone with benzaldehyde under various reaction conditions.

The obvious catalytic role of MNPs-IT-PA in Knoevenagel condensation could be attributed two points. As depicted in Fig.7, the nitrogen with a long pair electron at the primary amine of MNPs-IT-PA (Function domain) could be as a acceptor to form a hydrogen bond with methylene active ingredient. The resulted carbon anion would attack the aldehyde, followed by the removal of a molecular of  $\text{H}_2\text{O}$  to provide the final condensation product. Secondly, the hydrophilic domain of ionic moiety in the catalyst play a role as phase transfer catalyst (PTC), which

increased the solubility of reagent in water. It is clear that the poor water solubility of methylene active compound lead to the decrease in the catalytic activity of primary amine, verified by ionic-free  $\text{SiO}_2@\text{Fe}_3\text{O}_4$ -PA promoted processes (Table 1, entry 2 vs. entry 3 and Scheme 3, condition **A** vs. condition **B**). Moreover, the “ionic environment” present electrosteric activation to stabilize the transition state of reaction [15]. Both the hydrophobic property and good acceptor of nitrogen of MNPs-IT-PA facilitate the reaction efficiently.

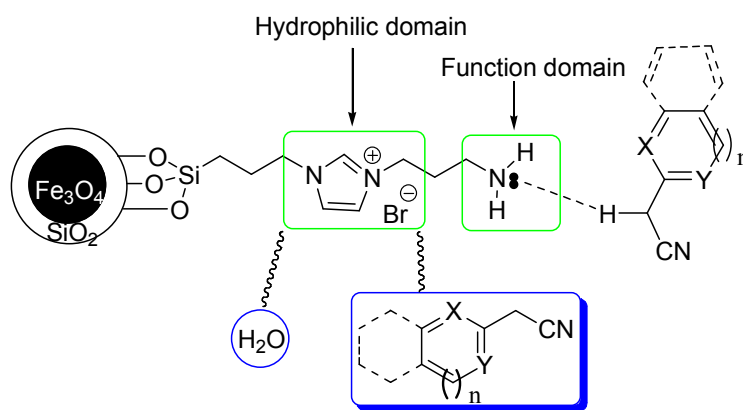


**Fig.7** Proposed explanation of MNPs-IT-PA as catalyst for Knoevenagel condensation.

One of the main advantages of the supported catalyst is its recyclability. Thus, we turned our attention to the reusability of the ionic tagged catalyst MNPs-IT-PA. Upon the completion of the reaction, the magnetic catalyst was readily recovered by an external magnet (Fig.5, b), and was reused in the next run before it was washed with ethanol, ethyl acetate, respectively. As shown in Fig.8, the catalyst MNPs-IT-PA could be reused for 8 times and no significant decrease in the product yield was observed. In addition, the amine loading regarding the catalyst subjected 8 times recyclability was 0.31 mmol/g, demonstrating the covalently connection between ionic modified amine and MNPs..

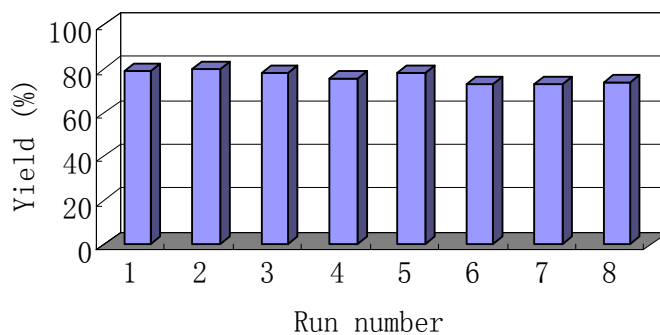


**Fig.8** Recycle study of the catalyst MNPs-IT-PA in the aqueous reaction of 2-(cyanomethyl)benzimidazole (5 mmol) and 2-thenaldehyde (5 mmol) in water (10 mL) within 2 h.

### 3. Conclusions

In conclusion, the first magnetic nanoparticles supported propylamine with an IL modification was designed and prepared. The ionic tagged supported catalyst MNPs-IT-PA was used as highly and efficient promoter for the Knoevenagel condensation to afford the products in good yields. Moreover, MNPs-IT-PA could also be used as catalyst to prepare 4-methyl-3-oxo-*N*-phenyl-2-(phenylmethylene)pentanamide, a key intermediate for the synthesis of Atorvastatin calcium. The comparison between MNPs-IT-PA and MNPs-PA shows that the ionic moiety facilitate the reaction efficiently. The catalyst MNPs-IT-PA can be reused 8 times with slight loss of catalytic activity.

### 4. Experimental

#### 4.1 Materials and instruments

All chemical reagents were purchased without further purification. The reaction monitoring was

accomplished by thin layer chromatography (TLC) on gel F254 plates. Powder X-ray diffraction data were obtained Cu K $\alpha$  radiation. Fourier transform infrared spectroscopy (FT-IR) were recorded on a spectrometer using KBr pellets. Transmission electron microscopy (TEM) was performed with a instrument operating at 40-100 kV. The magnetic measurements were carried out in a vibrating sample magnetometer (VSM) at room temperature.  $^1\text{H}$  and  $^{13}\text{C}$  NMR were recorded on a spectrometer at 400 MHz and 100 MHz in  $\text{CDCl}_3$ , respectively. Chemical shifts were reported in parts per million ( $\delta$ ), relative to the internal standard of tetramethylsilane (TMS).

#### 4.2 Preparation of silica coated magnetic nanoparticle- $\text{SiO}_2@ \text{Fe}_3\text{O}_4$ **1** (MNPs)

Magnetic ( $\text{Fe}_3\text{O}_4$ ) nanoparticles were prepared by the coprecipitation [25].  $\text{FeCl}_3 \cdot 6\text{H}_2\text{O}$  (8.1 g, 0.03 mmol) and  $\text{FeCl}_2 \cdot 4\text{H}_2\text{O}$  (4.97 g, 0.025 mmol) were added to deionized water (100 mL) and sonicated until the salts dissolved completely. Thus, the transparent solution was heated at 85 °C with vigorous mechanically stirring under  $\text{N}_2$  atmosphere for 1 h. The pH value was then adjusted to 9 using the concentrated aqueous ammonia (25 wt %). The black precipitate was washed several times with deionized water until the pH value of the eluent decreased to 7. The coating of a layer of silica on the surface of the naked  $\text{Fe}_3\text{O}_4$  was achieved by sol-gel method [26]. The naked  $\text{Fe}_3\text{O}_4$  (1.0 g) was diluted with ethanol (200 mL) by ultrasonic irradiation. To this well dispersed magnetic nanoparticles solution, 6 mL concentrated  $\text{NH}_3 \cdot \text{H}_2\text{O}$  and 2 mL of tetraethoxysilane (TEOS) were added and stirred for further 24 h at room temperature. The resulting MNPs **1** was collected by an external magnet and washed with water until the solution was neutral, then, was washed with ethanol and diethyl ether, respectively, and dried under vacuum.

#### 4.3 Synthesis of the catalysts MNPs-IT-PA and MNPs-PA

##### Synthesis of MNPs-IT-PA **4**

To a solution of imidazole (6.8 g, 100 mmol) in dry toluene (100 mL), 3-chloropropyltriethoxysilane (24 mL, 100 mmol) was added in one portion. The reaction solution was refluxed 24 h under nitrogen protection. The mixture was evaporated under reduced pressure to remove the organic solvent. The residue was purified with neutral alumina column chromatography (eluent: ethyl acetate) to give the intermediate **2**. 1.0 g of SiO<sub>2</sub>@ Fe<sub>3</sub>O<sub>4</sub> **1** (MNPs) was dispersed in 20 mL dry toluene by sonication for 1 h, and then intermediate **2** (0.5 g) was added to the solution. After mechanical stirring under nitrogen atmosphere at reflux condition for 48 h, the solid was magnetically separated, and washed with ethanol, followed by dry under vacuum to afford Im-MNPs **3**. The resultant **3** (1.0 g) was dispersed in 50 mL dry ethanol with sonification for 1 h. 3-Bromopropylamine (0.27 g, 2.0 mmol) in 20 mL dry ethanol was added dropwise to the mixture and was further refluxed for 48 h with nitrogen protection. The solid catalyst MNPs-IT-PA **4** was collected by external magnetic force, and rinsed with ethanol, and then was dried under vacuum for 6 h. Finally, 0.96 g grey nanopartilces (MNPs-IT-PA, **4**) was obtained with a loading of 0.34 mmol/g by elemental analysis.

#### Synthesis of MNPs-PA **6**

0.5 g of Silica coated magnetic nanoparticles **1** (MNPs) was dispersed in dry toluene (30 mL) by ultrasonification for 5 min. (3-Aminopropyl)triethoxy silane (1.8 g) were added and the reaction mixture was refluxed for 12 h under N<sub>2</sub> atmosphere. The supported catalyst MNPs-PA **6** was obtained by magnetic separation and washed with ethanol, dried in a vacuum oven at 60 °C for 6 h. The loading of the catalyst was determined to be 0.21 mmol/g by elemental analysis.

#### NMR data for intermediate **2**

<sup>1</sup>H NMR (400 MHz, CDCl<sub>3</sub>): δ 0.46-0.50(m, 2H), 1.13-1.15(m, 9H), 1.81(t, *J*=8Hz, 2H), 3.74(t,

$J=7.2\text{Hz}$ , 6H), 3.86(t,  $J=7.2\text{Hz}$ , 2H), 6.84(d,  $J=1.2\text{Hz}$ , 1H), 6.96(s, 1H), 7.40(s, 1H);  $^{13}\text{C}$  NMR (100 MHz,  $\text{CDCl}_3$ ):  $\delta$  7.3, 18.2, 24.8, 49.0, 58.4, 118.7, 129.2, 137.1

#### 4.4 General procedure for the MNPs-IT-PA catalyzed ambient Knoevenagel condensation in water

Benzaldehyde (5 mmol), methylene active compound (5 mmol), and MNPs-IT-PA (735 mg) were mixed in water (10 mL). The mixture was allowed to react at room temperature for a rational time, which was decided by TLC. Separated from the reaction solution by magnet, the catalyst was washed with ethanol and ethyl acetate, followed by drying under vacuum, was reused for subsequent runs. The decanting solution was directly filtrated and the remained residue was purified with recrystallization using ethanol or column chromatography using petroleum ether/ethyl acetate as the eluent. The products were characterized by  $^1\text{H}$  NMR,  $^{13}\text{C}$  NMR.

NMR data for representative products

2-(1*H*-benzoimidazol-2-yl)-3-(thiophen-2-yl)acrylonitrile (Table 1, model reaction)

$^1\text{H}$  NMR (400 MHz,  $\text{CDCl}_3$ ):  $\delta$  7.15-7.22(m, 1H), 7.30-7.37(m, 2H), 7.50-7.52(m, 1H), 7.66-7.70(m, 2H), 7.76-7.77(m, 1H), 7.87-7.89(m, 1H), 8.63(s, 1H);  $^{13}\text{C}$  NMR (100 MHz,  $\text{CDCl}_3$ ):  $\delta$  98.1, 115.6, 115.7, 116.7, 123.6, 129.1, 134.5, 136.8, 137.0, 139.3, 147.6

2-(1*H*-benzoimidazol-2-yl)-3-phenylacrylonitrile (Table 2, Entry 1)

$^1\text{H}$  NMR (400 MHz,  $\text{CDCl}_3$ ):  $\delta$  7.31-7.34(m, 2H), 7.50-7.52(m, 3H), 7.65(s, 2H), 7.98-7.80(m, 2H), 8.51(s, 1H);  $^{13}\text{C}$  NMR (100 MHz,  $\text{CDCl}_3$ ):  $\delta$  111.2, 116.8, 119.7, 123.6, 124.2, 129.3, 130.0, 132.1, 132.7, 146.3, 146.8

2-(1*H*-benzoimidazol-2-yl)-3-(3-methoxyphenyl)acrylonitrile (Table 2, Entry 4)

$^1\text{H}$  NMR (400 MHz,  $\text{CDCl}_3$ ):  $\delta$  3.89(s, 3H), 7.07-7.09(m, 1H), 7.33-7.44(m, 3H), 7.55-7.59(m, 2H), 7.66(s, 2H), 8.53(s, 1H);  $^{13}\text{C}$  NMR (100 MHz,  $\text{CDCl}_3$ ):  $\delta$  55.5, 105.8, 114.1, 116.5, 119.0,

121.7, 123.4, 123.7, 126.0, 127.0, 130.2, 133.6, 135.0, 146.9, 153.6, 160.0, 162.7

2-(1*H*-indol-2-yl)-3-phenylacrylonitrile (Table 2, Entry 15)

<sup>1</sup>H NMR (400 MHz, CDCl<sub>3</sub>): δ 7.28-7.33 (m, 2H), 7.41-7.49 (m, 4H), 7.60-7.63 (m, 2H), 7.88 (d, 2H, *J*=5.6 Hz), 8.00 (d, 1H, *J*=6.0Hz), 8.58 (s, 1H); <sup>13</sup>C NMR (100 MHz, CDCl<sub>3</sub>): δ 106.5, 112.4, 113.1, 118.9, 120.0, 121.5, 123.6, 124.4, 125.8, 128.9, 129.1, 129.8, 134.9, 137.3, 138.2

2-(1*H*-indol-2-yl)-3-*p*-tolylacrylonitrile (Table 2, Entry 16)

<sup>1</sup>H NMR (400 MHz, CDCl<sub>3</sub>): δ 2.42(s, 3H), 7.26-7.33(m, 4H), 7.45(d, 1H, *J*=6.4Hz), 7.57-7.60(m, 2H), 7.79(d, 2H, *J*=6.4Hz), 8.00(d, 1H, *J*=6.0Hz), 8.46(s, 1H); <sup>13</sup>C NMR (100 MHz, CDCl<sub>3</sub>): δ 21.8, 105.3, 112.3, 113.3, 119.1, 120.0, 121.4, 123.5, 124.4, 125.4, 128.9, 129.8, 132.1, 137.2, 138.5, 140.2

4-Methyl-3-oxo-*N*-phenyl-2-(phenylmethylene)pentanamide (Scheme 3, **II**)

<sup>1</sup>H NMR (400 MHz, CDCl<sub>3</sub>): δ 1.21(d, 6H, *J*=6.4Hz), 3.36(m, 1H), 7.14-7.18(m, 1H), 7.32-7.38(m, 5H), 7.47(d, 2H, *J*=7.6Hz), 7.56-7.59(m, 3H), 7.64(s, 1H); <sup>13</sup>C NMR (100 MHz, CDCl<sub>3</sub>): δ 19.1, 36.7, 120.3, 125.0, 129.0, 129.1, 130.0, 130.1, 133.0, 136.2, 137.4, 140.7, 165.5.

## Acknowledgements

We are grateful for the financial supports for this research by the National Natural Science Foundation of China (Grant 21106090 and 21272169), Foundation of Low Carbon Fatty Amine Engineering Research Center of Zhejiang Province (2012E10033), and Zhejiang Provincial Natural Science Foundation of China (No. LY12B02004 and LQ13B070002).

## References

- [1] D. T. Mowry, *J. Am. Chem. Soc.* **1945**, *67*, 1050.
- [2] R. Trotski, M. M. Hoffmann, B. Ontruschka, *Green Chem.* **2008**, *10*, 873.
- [3] Y.-F. Lai, H. Zheng, S.-J. Chai, P.-F. Zhang, X.-Z. Chen, *Green Chem.* **2010**, *12*, 1917.
- [4] W. Yu, S. Zhang, S. Ying, C. Zhao, S. Luo, C. Au, *Catal. Commun.* **2011**, *12*, 1333.
- [5] C. Mukhopadhyay, S. Ray, *Catal. Commun.* **2011**, *12*, 1496.
- [6] M. Zhang, P. Zhao, Y. Leng, G. Chen, J. Wang, J. Huang, *Chem. Eur. J.* **2012**, *18*, 12773.
- [7] (a) A. Dandia, V. Parewa, A. K. Jain, K. S. Rathore, *Green Chem.* **2011**, *13*, 2135. (b) S. Sobhani, Z. P. Parizi, S. Rezazadeh, *J. Organometallic Chem.* **2011**, *696*, 813. (c) L. Tedeschi, D. Enders, *Org. Lett.* **2011**, *3*, 3515.
- [8] (a) L. E. Polander, S. Barlow, B. M. Seifried, S. R. Marder, *J. Org. Chem.* **2012**, *77*, 9426. (b) J. Mondal, A. Modak, A. Bhaumik, *J. Mol. Catal. A: Chem.* **2011**, *355*, 236. (c) S. B. Bharate, R. Mudududdla, J. B. Bharate, N. Battini, S. Battula, R. R. Yadav, B. Singh, R. A. Vishwakarma, *Org. Biomol. Chem.* **2012**, *10*, 5143. (d) J. Wang, Z. Zhang, W. Wang, F. Liu, *Org. Biomol. Chem.* **2013**, *11*, 2034.
- [9] (a) F. Liang, Y.-J. Pu, T. Kurata, J. Kido, H. Nishide, *Polymer* **2005**, *46*, 3767. (b) G. A. Kraus, M. E. Krolski, *J. Org. Chem.* **1986**, *51*, 3347. (c) F. Freeman, *Chem. Rev.* **1980**, *80*, 329.
- [10] (a) A. V. Narsaiah, A. K. Basak, B. Visali, K. Nagaiah, *Synth. Commun.* **2004**, *34*, 2893. (b) J. J. Han, Y. F. Xu, Y. P. Su, X. G. She, X. F. Pan, *Catal. Commun.* **2008**, *9*, 2077.
- [11] (a) M. B. Gawande, R. V. Jayaram, *Catal. Commun.* **2006**, *7*, 931. (b) G. Li, J. Xiao, W. Zhang, *Green Chem.* **2012**, *14*, 2234. (c) G. Li, J. Xiao, W. Zhang, *Green Chem.* **2011**, *13*, 1828. (d) Y. Wei, S. Zhang, S. Yin, C. Zhao, S. Luo, C. Au, *Catal. Commun.* **2011**, *12*, 1333. (e) V. S. R. R. Pullabhotla, A. Rahman, S. B. Jonnalaghadda, *Catal. Commun.* **2009**, *10*, 365. (f) L.

- Martins, W. Hölderich, P. Hammer, D. Cardoso, *J. Catal.* **2010**, *271*, 220. (g) F. X. L. Xamena, F. G. Cirujano, A. Corma, *Microporous Mesoporous Mater.* **2012**, *157*, 112.
- [12] See recently published reviews: (a) A. H. Lu, E. L. Salabas, F. Schüth, *Angew. Chem. Int. Ed.* **2007**, *46*, 1222. (b) M. B. Gawande, P. S. Branco, R. S. Varma, *Chem. Soc. Rev.* **2013**, *42*, 3371. (c) R. B. Nasir Baig, R. S. Varma, *Chem. Commun.* **2013**, *49*, 752.
- [13] B. Atashkar, A. Rostami, B. Tahmasbi, *Catal. Sci. Technol.* **2013**, *3*, 2140.
- [14] M. B. Gawande, A. K. I. D. Rathi, Nogueira, R. S. Varma, P. S. Branco, *Green Chem.* **2013**, *15*, 1895.
- [15] M. Lombardo, C. Trombini, *ChemCatChem* **2010**, *2*, 135.
- [16] A. Ying, S. Liu, Y. Ni, F. Qiu, S. Xu, W. Tang, *Catal. Sci. Technol.* **2014**, *4*, 2115.
- [17] X. Jin, D. Yang, X. Xu, Z. Yang, *Chem. Commun.* **2012**, *48*, 9017.
- [18] M. R. dos Santos, A. F. Gomes, F. C. Gozzo, P. A. Z. Suarez, B. A. D. Neto, *ChemSusChem* **2012**, *5*, 2383.
- [19] M. Lombardo, M. Chiarucci, C. Trombini, *Green Chem.* **2009**, *11*, 574.
- [20] Z.-H. Li, Z.-M. Zhou, X.-Y. Hao, J. Zhang, X. Dong, Y.-Q. Liu, *Chirality* **2012**, *24*, 1092.
- [21] S. S. Khan, J. Shah, J. Liebscher, *Tetrahedron* **2011**, *67*, 1812.
- [22] L. Dai, H. Yuan, X. Li, Z. Li, D. Xu, F. Fei, Y. Liu, J. Zhang, *Tetrahedron: Asymmetry* **2011**, *22*, 1379.
- [23] M. Lombardo, M. Chiarucci, C. Trombini, *Chem. Eur. J.* **2008**, *14*, 11288.
- [24] (a) A. Ying, S. Xu, S. Liu, Y. Ni, J. Yang, C. Wu, *Ind. Eng. Chem. Res.* **2014**, *53*, 547. (b) A. Ying, H. Liang, R. Zheng, C. Ge, H. Jiang, C. Wu, *Res. Chem. Intermed.* **2011**, *37*, 579. (c) A.-G. Ying, L. Liu, G.-F. Wu, G. Chen, X.-Z. Chen, W.-D. Ye, *Tetrahedron Lett.* **2009**, *50*,

1653. (d) A.-G. Ying, X.-Z. Chen, C.-L. Wu, R.-H. Zheng, H.-D. Liang, C.-H. Ge, *Synth. Commun.* **2012**, *42*, 3455. (e) A. Ying, Y. Ni, S. Xu, S. Liu, J. Yang, R. Li, *Ind. Eng. Chem. Res.* **2014**, *53*, 5678. (f) S. Liu, Y. Ni, J. Yang, H. Hu, A. Ying, S. Xu, *Chin. J. Chem.* **2014**, *32*, 343.
- [25] (a) K. Nishioa, M. Ikedaa, N. Gokonb, S. Tsubouchi, H. Narimatsua, Y. Mochizuki, S. Sakamotoa, A. Sandhuc, M. Abe, H. Handa, *J. Magn. Magn. Mater.* **2007**, *310*, 2408. (b) Y. Jiang, C. Guo, H. Gao, H. Xia, I. Mahmood, C. Liu, H. Liu, *AIChE J.* **2012**, *58*, 1203.
- [26] Y. H. Deng, D. W. Qi, C. H. Deng, X. M. Zhang, D. Y. Zhao, *J. Am. Chem. Soc.* **2008**, *130*, 28.
- [27] (a) A. L. Morel, S. I. Nikitenko, K. Gionnet, A. Wattiaux, J. Lai-Kee-Him, C. Labrugere, B. Chevalier, G. Deleris, C. Petibois, A. Brisson, M. Simonoff, *ACS Nano* **2008**, *2*, 847. (b) Q. Zhang, H. Su, J. Luo, Y. Wei, *Green Chem.* **2012**, *14*, 201. (c) Q. Du, W. Zhang, H. Ma, J. Zheng, B. Zhou, Y. Li, *Tetrahedron* **2012**, *68*, 3577.
- [28] (a) X. Wang, P. P. Dou, P. Zhao, C. M. Zhao, Y. Ding, P. Xu, *ChemSusChem* **2009**, *2*, 947. (b) H.-J. Xu, X. Wan, Y.-Y. Shen, S. Xu, Y.-S. Feng, *Org. Lett.* **2012**, *14*, 1210.
- [29] Y. Zhang, Y. Zhao, C. Xia, *J. Mol. Catal. A: Chem.* **2009**, *306*, 107.
- [30] A. Bordoloi, S. Sahoo, F. Lefebvre, S. B. Halligudi, *J. Catal.* **2008**, *259*, 232.
- [31] F. Nemati, M. M. Heravi, R. S. Rad, *Chin. J. Catal.* **2012**, *33*, 1825.
- [32] G. Wang, N. Yu, L. Peng, R. Tan, H. Zhao, D. Yin, H. Qiu, Z. Fu, D. Yin, *Catal. Lett.* **2008**, *123*, 252.
- [33] Y. Kong, R. Tan, L. Zhao, D. Yin, *Green Chem.* **2013**, *15*, 2422.
- [34] (a) A. Graul, J. Castaner, *Drugs Future* **1997**, *22*, 956; (b) K. L. Baumann, D. E. Butler, C. F.

Deering, K. E. Mennen, A. Millar, T. N. Nanninga, C. W. Palmer, B. D. Roth, *Tetrahedron Lett.* **1992**, *33*, 2283; (c) H. W. Lee, Y. M. Kim, C. L. Yoo, S. K. Kang, S. K. Ahn, *Biomolecules & Therapeutics* **2008**, *16*, 28.